33rd Annual International Conference of the IEEE EMBS
Boston, Massachusetts USA, August 30 - September 3, 2011

Continuous Decoding of Intended Movements with a Hybrid Kinetic and Kinematic Brain Machine Interface

Aaron J. Suminski, *Member, IEEE*, Francis R. Willett, Andrew H. Fagg, *Member, IEEE*, Matthew Bodenhamer, and Nicholas G. Hatsopoulos

***Abstract*—Although most brain–machine interface (BMI) studies have focused on decoding kinematic parameters of motion, it is known that motor cortical activity also correlates with kinetic signals, including hand force and joint torque. In this experiment, a monkey used a cortically-controlled BMI to move a visual cursor and hit a sequence of randomly placed targets. By varying the contributions of separate kinetic and kinematic decoders to the movement of a virtual arm, we evaluated the hypothesis that a BMI incorporating both signals (Hybrid BMI) would outperform a BMI decoding kinematic information alone (Position BMI). We show that the trajectories generated by the Hybrid BMI during real-time decoding were straighter and smoother than those of the Position BMI. These results may have important implications for BMI applications that require controlling devices with inherent, physical dynamics or applying forces to the environment.**

I. Introduction

Most brain-machine interfaces (BMI) to date have focused solely on decoding kinematic variables, such as hand position or velocity, in order to infer the intended movement trajectory of the user (e.g. [1]-[3]). However, a number of studies have provided evidence that the primary motor cortex (MI) encodes kinetic signals as well, including hand force and joint torque [4]-[6]. Use of these kinetic signals could improve upon the performance of kinematic decoders and may be necessary to extend the applicability of these BMIs to more complex tasks, such as picking up objects of varying mass. A recent study confirmed the possibility of decoding a kinetic signal, showing that elbow and shoulder joint torques can be reconstructed with accuracy nearly equivalent to that of a hand position signal [7].

Here, we sought to improve BMI performance by simultaneously decoding intended joint torques and hand position from a monkey's neural signals in MI. These two signals were used to drive a simulated two-link arm, whose position was communicated visually to the monkey as the position of a cursor on a screen. In all the configurations we tested, the combination of kinetic and kinematic decoders during real-time BMI control resulted in movements that were straighter and smoother than those of a kinematic decoder.

Manuscript received April 15, 2011. This work was supported by NIH NINDS R01 N545853-01 to NGH and AHF.

A. J. Suminski is with the Department of Organismal Biology and Anatomy at the University of Chicago, Chicago, IL 60637 USA (asuminski@uchicago.edu).

F. R. Willett is with the Department of Organismal Biology and Anatomy at the University of Chicago, Chicago, IL 60637 USA (fwillett@uchicago.edu).

A. H. Fagg is with the School of Computer Science at the University of Oklahoma, Norman, OK 73019 USA (fagg@cs.ou.edu).

M. Bodenhamer is with the School of Computer Science at the University of Oklahoma, Norman, OK 73019 USA (mbodenhamer@cs.ou.edu).

N. G. Hatsopoulos is with the Department of Organismal Biology and Anatomy and the Committee on Computational Neuroscience at the University of Chicago, Chicago, IL 60637 USA (nicho@uchicago.edu).

II. Methods

A. Behavioral Task

One adult male rhesus macaque (*Macaca mulatta*) was trained to control a cursor in a two–dimensional workspace using the KINARM, a two-link robotic exoskeleton (BKIN Technologies, Kingston, ON). The animal sat in a primate chair with his arm abducted 90 degrees and supported by the robot such that all movements were made within the horizontal plane. Direct vision of the arm was precluded by a horizontal projection screen. Visual feedback was available via a cursor projected onto the screen. The position of the cursor was controlled by one of two sources: either the position of the robot's end effector (i.e. the monkey's hand position) or the output of a BMI that decoded the position of the cursor based on neural activity in the recent past.

The random target pursuit (RTP) task required the monkey to repetitively move a cursor (6 mm diameter) to a square target ($2.25cm^2$). The target appeared at a random location within the workspace (12 cm by 12 cm), and each time the monkey hit it, a new target appeared immediately in a random location. This task was designed to generate complex movements that thoroughly sample the position and velocity space of the arm. In order to complete a successful trial the monkey was required to sequentially acquire either three targets (BMI conditions) or seven targets (Active Movement). A trial was aborted if any movement between targets took longer than 2.5s.

B. Real-Time Hybrid BMI

Our Hybrid BMI (Figure 1) converts neural activity into elbow and shoulder joint torques in order to drive the movement of a two-link simulated arm. The hand position of the simulated arm (X_C) is updated based on the current joint angles, velocities, and accelerations of the virtual arm and the joint torques generated by the BMI (τ). The torques, τ,

are a weighted combination of the torques generated by the individual components of the Hybrid BMI:

$$\tau = Kt * \tau_t + Kp * \tau_p + Kv * \tau_v , \quad (1)$$

where τ_t is the prediction of the monkey's intended shoulder and elbow joint torques made by the torque decoder, τ_p is the torque generated by the position controller, τ_v is the torque generated by the velocity controller, and Kt, Kp, and Kv are gain coefficients to control the mixture of the component torques.

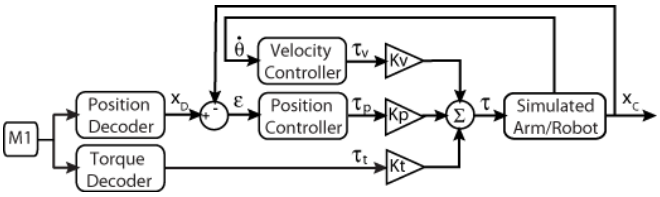

Figure 1: The Hybrid BMI uses neural activity recorded from the primary motor cortex to generate a simulated hand position in Cartesian space which the monkey then uses to hit targets. X_D and X_C are two-element column vectors containing the X and Y components of a hand position in Cartesian space, ε is a two-element column vector containing the X and Y components of an error signal, τ_t, τ_p, τ_v and τ are two-element column vectors containing joint torque terms, and Kt, Kp, and Kv are scalar gating terms.

The position and velocity controllers function together as a PD-controller to move the simulated arm towards the position decoder's prediction of the monkey's intended hand position, X_D. The position controller uses the error signal, $\varepsilon = X_D - X_C$, to generate τ_p according to (2):

$$\tau_p = \begin{bmatrix} P_s & 0 \\ 0 & P_e \end{bmatrix} J^{-1} \begin{bmatrix} \varepsilon_x \\ \varepsilon_y \end{bmatrix}, \quad (2)$$

where J^{-1} is the 2x2 inverse Jacobian for the KINARM, ε_x and ε_y are position errors in the X and Y direction and P_s and P_e are constant gain parameters. Similarly, the velocity controller generates joint torques proportional to the current angular velocities of the simulated arm according to (3):

$$\tau_v = \begin{bmatrix} D_s & 0 \\ 0 & D_e \end{bmatrix} \begin{bmatrix} d\theta_s/dt \\ d\theta_e/dt \end{bmatrix}, \quad (3)$$

where $d\theta_s/dt$ and $d\theta_e/dt$ are the angular velocities of the shoulder and elbow, D_s and D_e are constant gain parameters. P_s, P_e, D_s and D_e were tuned in simulation prior to the experiments.

The position and torque decoders, implemented as Wiener Filters, predict the monkey's intended hand position, X_D, and the monkey's intended joint torque, τ_t. In our approach, an estimate of "intended" hand position/joint torque is reconstructed from a linear combination of binned spike counts from the available neurons. We employ a history of B = 20 bins of Δt = 50ms each for every neuron, giving the Wiener Filters access to a total of one second of neural spiking history. Specifically, signal k (X or Y hand position, or elbow or shoulder torque) at discrete time bin t, is reconstructed as follows:

$$S(t,k) = \sum_{j=0}^{B-1} \sum_{i=0}^{C-1} A(k, j+iB) \times N(i, t-j) , \quad (4)$$

where i indexes over the C neurons, j indexes over time bins, Δt = 50ms is the bin size, $N(i, t)$ is the spike count of neuron i over time bin t, and A are the coefficients.

As in our previous work, the coefficients for the decoder are solved for analytically using ridge regression that trades prediction accuracy on the training set for a smoother prediction surface [8]. Specifically, given T paired observations of spike counts N and signal S (of dimensionality $C \times T$ and $L \times T$, respectively), we first construct a matrix M where each column represents one second of recent neural activity for each available cell at a given time point:

$$M = \begin{bmatrix} N(0,0) & N(0,1) & \cdots & N(0,T-20) \\ N(0,1) & N(0,2) & \cdots & N(0,T-19) \\ \vdots & \vdots & \ddots & \vdots \\ N(0,19) & N(0,20) & \cdots & N(0,T-1) \\ N(1,0) & N(1,1) & \cdots & N(1,T-20) \\ \vdots & \vdots & \ddots & \vdots \\ N(C-1,19) & N(C-1,20) & \cdots & N(C-1,T-1) \end{bmatrix}, \quad (5)$$

and a matrix $\hat{S}$, where each column represents the set of signals to be predicted given the information contained in the corresponding column of M:

$$\hat{S} = \begin{bmatrix} S(0,19) & S(0,20) & \cdots & S(0,T-1) \\ S(1,19) & S(1,20) & \cdots & S(1,T-1) \\ \vdots & \vdots & \ddots & \vdots \\ S(L-1,19) & S(L-1,20) & \cdots & S(L-1,T-1) \end{bmatrix}. \quad (6)$$

The coefficients are solved for as follows:

$$A^T = (M\ M^T + \alpha I)^{-1} M\ \hat{S}^T , \quad (7)$$

where α is a regularization parameter that controls the tradeoff between explaining the training data set and smoothness.

The simulated arm is a two-link arm model that represents the monkey's arm in the KINARM robotic exoskeleton. The forward and inverse dynamics equations for the KINARM and the monkey's arm have been described previously [7]. The mass and rotational inertia terms in the model are based on anatomical models of rhesus macaques [9] and measurements from our monkey and the KINARM.

C. Experimental Procedure

Prior to all experiments, the monkey used its arm to perform the RTP task (Active Movement, AM). While the animal performed this task, we recorded four minutes (4800, 50ms bins) of spiking activity and movement data to train two decoders that predict cursor position or joint torque. The torques used to train the decoder were estimated from the observed arm trajectories and an inverse dynamics model that included both the KINARM and the monkey arm.

During the experiments, the monkey used a BMI to move the cursor in the same task based on the activity of an ensemble of recorded motor cortical neurons. The monkey was free to move his arm during the BMI conditions.

We performed two sets of experiments to explore the behavior of the Hybrid BMI under various configurations. We fixed the value of Kv to 0.1 for all experiments in order to reduce the size of the parameter space. We chose Kv such that it allowed us to explore combinations of Kt and Kp where τ_t and τ_p made similar contributions to the movement of the simulated arm.

In the first experiments, we were interested in determining the combination of Kt and Kp that yielded the best BMI performance. First, we eliminated the contribution of the torque decoder (Position BMI, Kt = 0) and varied the magnitude of Kp from 0.05 to 1. Next, we fixed Kp at its best value (0.2) and varied Kt from 0 to 4 (Hybrid BMI) in order to determine the combination of Kp and Kt yielding the best BMI performance. In both experiments, the monkey performed approximately 50 trials in each session for each value of Kp or Kt.

Next, we performed experiments designed to directly test the hypothesis that the Hybrid BMI would improve BMI performance relative to the Position BMI even at suboptimal Kp values. These experiments consisted of four conditions: Active Movement, Position BMI, Hybrid BMI and Direct Position BMI. During the Direct Position BMI condition the visual cursor position was controlled by the output of the position decoder, X_D, instead of the hand position of the simulated arm. Each BMI condition was presented randomly in blocks of 50 trials following an initial block of the Active Movement condition.

D. Electrophysiology

The monkey was chronically implanted with a 100-electrode microelectrode array (Blackrock Microsystems, Inc., Salt Lake City, UT) in MI contralateral to the arm used for the task. The electrodes on the array were 1.5 mm in length and were coated with iridium oxide. During each recording session, signals from up to 96 electrodes were amplified (gain of 5000), band-pass filtered between 0.3 Hz and 7.5 kHz, and recorded digitally (14-bit) at 30 kHz per channel using a Cerebus acquisition system (Blackrock Microsystems, Inc., Salt Lake City, UT). Only waveforms that crossed a user defined threshold were used for real-time decoding. The neural data used to train and drive the BMI during the experiments were comprised of single and multiunit spiking events that were sorted online. On average, 52.45 ± 1.12 (mean ± 1 standard error) neural channels were sampled during each BMI session. All of the surgical and behavioral procedures were approved by the University of Chicago Institutional Animal Care and Use Committee and conform to the principles outlined in the *Guide for the Care and Use of Laboratory Animals*.

E. Kinematic Analyses

To assess performance differences between the BMI conditions, we used two kinematic measures: 1) normalized time-to-target, and 2) normalized path length. The normalized time-to-target metric is defined as the time difference between consecutive target hits divided by the Euclidean distance between the targets. The normalized path length metric is defined as the path length of the cursor between consecutive targets divided by the Euclidean distance between consecutive targets.

III. Results

We sought to demonstrate that the performance of a BMI decoding both kinematic and kinetic movement variables was superior to that of a kinematic controller alone. We determined the combination of Kp and Kt that yielded the best task performance by first finding the best performing Position BMI (i.e. varying the magnitude of Kp while holding Kt = 0). Examination of the cursor trajectories generated by the various Position BMIs showed that, as Kp increased, the time between consecutive target hits decreased (i.e. increased performance) and the relative length of the movement paths increased (i.e. movements became increasingly jerky) as shown in Fig. 2a. This tradeoff between movement speed and path straightness combined with qualitative observations of the monkey's behavior led us to conclude that an intermediate value of Kp = 0.2 would provide the best compromise between straight and fast movements. Next, we fixed Kp = 0.2 and varied Kt in order to determine the combination of kinetic and kinematic controllers yielding the best task performance (Fig 2b). Similar to our observations when varying Kp, the time between target hits decreased as Kt increased. The cursor trajectories, however, straightened as Kt increased, reaching a minimum at Kt = 1.4 before becoming increasingly jerky as Kt grew larger. This suggested the best Hybrid BMI for Kp = 0.2 occurs at Kt = 1.4. We quantified the contribution of the position controller (τ_p) and torque decoder (τ_t) to the total torque (τ) generated by the Hybrid BMI by computing the ratio of root mean square torques from each part of the hybrid system, $RMS\tau_p/RMS\tau_t$. This specific combination of parameters (Kp = 0.2, Kt = 1.4) resulted in a ratio of 1.64.

Based on the results of the first experiments, we wished to compare the best Hybrid and Position BMIs (Kp = 0.2) directly. However, due to the ambiguity in selecting the best Position BMI (Fig. 2a), we also performed separate experiments comparing the Position BMI and Hybrid BMI where Kp = 0.1 and 0.4. For these values of Kp, we estimated the values of Kt such that the ratio $RMS\tau_p/RMS\tau_t$ would be similar to that observed for the best Hybrid BMI. This computation yielded Hybrid BMIs with parameters Kp = 0.1, Kt = 0.9 and Kp = 0.4, Kt = 2.2 having $RMS\tau_p/RMS\tau_t$ ratios of 1.71 and 1.65, respectively.

The monkey was able to perform the RTP task successfully using both the Position and Hybrid BMIs,

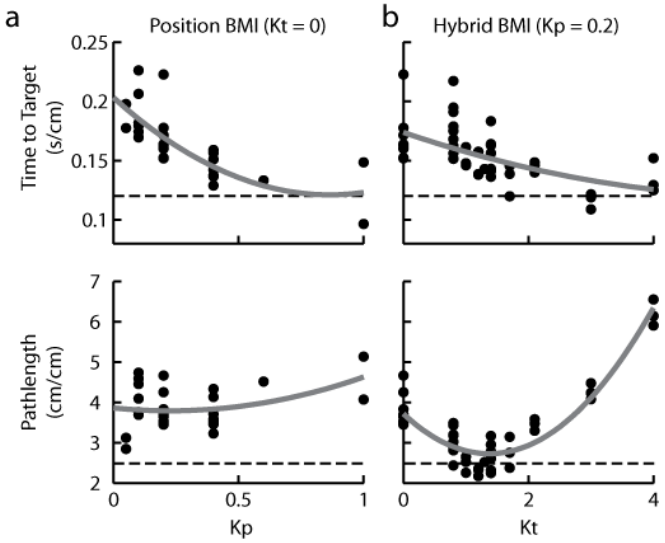

Figure 2: (a) Performance metrics for Position BMIs (Kt = 0) as a function of Kp. Each black dot represents the mean performance over all reaches of a particular controller for one particular day on which it was tested. (b) Same metrics as in (a) plotted for Hybrid BMIs with Kp = 0.2 and a variable Kt. The data were fit by a quadratic model for each metric (gray line). The black dashed line represents performance in the active movement condition.

achieving at least an 80% success rate (Table 1). Consistent with our hypothesis, we found that at least one of the performance measures improved in all cases when the monkey used the Hybrid BMI. The mean normalized path length decreased significantly in all the Hybrid BMI conditions compared to the corresponding Position BMI ($p < 0.05$, two sample t-test). The monkey also generated faster target to target movements using the Hybrid BMI at Kp = 0.1 ($p < 0.05$, two sample t-test). There was no difference in the mean time to target for the Hybrid and Position BMIs at Kp = 0.2 and 0.4 ($p > 0.05$).

Similarly, the monkey was able to use the Direct Position BMI to perform the RTP task. We included this condition in order to compare the Hybrid BMI to traditional kinematics based BMIs. A qualitative comparison of these BMIs reveals that the Direct Position and Hybrid BMIs perform similarly in both the mean time to target and path length metrics. This comparison, however, is not fair in that the Hybrid BMI controls the movement of the virtual arm, while the Direct Position BMI only moves a massless cursor.

We reconstructed the simulated arm movements of the Hybrid and Position BMIs offline to illustrate the tradeoff in path length and time to target that we observed when we varied Kp (Fig. 3). Here, the neural data recorded during Active Movement and the position and torque decoders (built on the same day) were used to compute the decoded hand position X_D and the decoded torques τ_t. Given these inputs, we then integrated the forward dynamics model in time to produce simulated BMI trajectories. The high frequency components in the position and torque time series of the Position BMI illustrate the tradeoff. Though the monkey was able to acquire targets quickly online (Fig. 2a, Kp = 1), the increased path length, due to rapid changes in torque, made this particular Position BMI ultimately undesirable. By comparison, the best Hybrid BMI (Kp = 0.2, Kt = 1.4) produced smoothly varying torques resulting in straighter movements.

TABLE I
PERFORMANCE METRICS FOR REACHES DURING THE ACTIVE AND BMI MOVEMENTS

	Time to Target (s/cm)	Path Length (cm/cm)	Success Rate (%)
AM	0.118 ± 0.0007	2.46 ± 0.01	95.7 ± 0.9
Direct Position BMI	0.154 ± 0.0024	2.89 ± 0.04	85.7 ± 3.3
Position BMI (0.1)	0.178 ± 0.0042	4.18 ± 0.11	79.2 ± 3.6
Hybrid BMI (0.1)	0.157 ± 0.0028	2.39 ± 0.04	87.1 ± 4.9
Position BMI (0.2)	0.170 ± 0.0035	3.72 ± 0.08	84.8 ± 0.6
Hybrid BMI (0.2)	0.164 ± 0.0026	2.89 ± 0.05	89.6 ± 1.7
Position BMI (0.4)	0.156 ± 0.0137	4.34 ± 0.35	96.8
Hybrid BMI (0.4)	0.156 ± 0.0118	3.45 ± 0.26	92.4

All values reported are mean ± 1 SEM. The value of Kp is indicated by the quantity in parentheses in condition titles [e.g. Hybrid BMI (0.2)]. Data in the Kp = 0.4 conditions were collected in a single session.

IV. DISCUSSION

Our results demonstrate the utility of decoding kinetic variables for real-time BMI control. In all the configurations we tested, the combination of kinetic and kinematic decoders in a Hybrid BMI resulted in cursor movements that were straighter and smoother than those observed using a Position BMI. Interestingly, we found that the $RMS\tau_p/RMS\tau_t$ ratios for the best Hybrid BMIs we tested were greater than 1 (ranging from 1.64 to 1.71) indicating a larger contribution of the position controller. Performance data showed that when the decoded torque became too large, the quality of movement degraded even though targets were acquired quickly. When Kt = 2.2, 3 and 4 (Fig. 2b), we observed a sharp increase in the path length due to oscillations in the hand trajectories. These oscillations were likely induced by large position errors resulting from the heavy influence of the τ_t torques.

We should note that the optimum set of Kp, Kd, and Kt parameters will depend on the individual monkey. Because each monkey has different arm lengths and segment masses, the virtual arm model will be different for each monkey and will behave differently in response to the same joint torques. In future work we plan to use an offline optimization approach to estimate the optimum values for any given monkey. This strategy will allow us to avoid the process of experimentally exploring the parameter space for each new monkey.

Our explorations of the Hybrid BMI parameter space were somewhat limited in scope because we fixed the four parameters of the PD controller (P_s, P_e, D_s and D_e; see equations 2 and 3) and manipulated only Kp and Kd. In addition, we set the value of Kd at 0.1 in an attempt to balance the torques generated by the position controller and torque decoder. Although this constraint helped us to find

good Hybrid BMIs, it also made Position BMIs with larger values of Kp less viable because they were underdamped. In future work we plan to eliminate the constraint on Kd and to allow our Position and Hybrid BMIs to use different sets of PD parameters optimized in offline simulations. This will allow Position BMIs to use larger PD parameters, while the Hybrid BMI will be able to use smaller parameters to maximize the contribution of the torque decoder.

Our work is limited in that we tested the Hybrid and Position BMIs in one dynamic context. Future work will involve testing the ability of these BMIs to adapt to different dynamic contexts. The simulated arm included in the Hybrid BMI allows us to test the ability of a BMI to adapt its dynamic output according to the demands of the task.

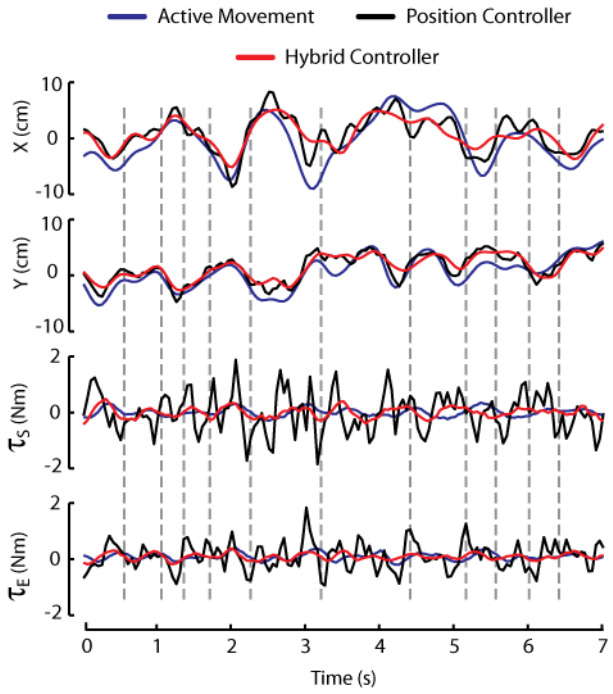

Figure 3: Time series comparing movements in the Active Movement condition (blue line) to offline reconstructions of simulated arm position using the Hybrid (red line; Kp = 0.2, Kt = 1.4) and Position (black line; Kp = 1, Kt = 0) BMIs. The Cartesian position and joint torque of either the monkey's arm or the simulated arm are represented by X, Y, τ_s and τ_e. Dashed lines show the times at which a target was hit during Active Movement. Note the large, high frequency torques generated by the Position BMI and the small reversals in the movement trajectories that result.

Although we showed that the monkey was successfully able to use the Position BMI with no contribution from the torque decoder, it is interesting to note that the monkey was unable to perform the task using a pure Torque BMI (i.e. Kt = 1.0, Kp = 0). We believe that this demonstrates that a Torque BMI is radically different from one having a strong position component. Further investigations of a Torque BMI may require a behavioral task requiring precise control of joint torque allowing the monkey to make a seamless transition from normal behavior to Torque BMI control.

REFERENCES

[1] J.Wessberg, C. R. Stambaugh, J. D. Kralik, P. D. Beck, M. Laubach, J. K. Chapin, J. Kim, S. J. Biggs, M. A. Srinivasan, and M. A. Nicolelis, "Real-time prediction of hand trajectory by ensembles of cortical neurons in primates," *Nature*, vol. 408, pp. 361–5, 2000.

[2] M. D. Serruya, N. G. Hatsopoulos, L. Paninski, M. R. Fellows, and J. P. Donoghue, "Instant neural control of a movement signal," *Nature*, vol. 416, pp. 141–2, 2002.

[3] D. M. Taylor, S. I. Tillery, and A. B. Schwartz, "Direct cortical control of 3D neuroprosthetic devices," *Science*, vol. 296, pp. 1829–32, 2002.

[4] M.-C. Hepp-Reymond, U. R.Wyss, and R. Anner, *Neuronal Coding of Static Force in the Primate Motor Cortex*, vol. 74, pp. 287–291, 1978.

[5] P. D. Cheney and E. E. Fetz, "Functional classes of primate corticomotoneuronal cells and their relation to active force," *J. Neurophysiol.*, vol. 44, pp. 773–91, 1980.

[6] D. W. Cabel, P. Cisek, and S. H. Scott, "Neural activity in primary motor cortex related to mechanical loads applied to the shoulder and elbow during a postural task," *J. Neurophysiol.*, vol. 86, pp. 2102–8, 2001

[7] A. H. Fagg, G. W. Ojakangas, L. E. Miller, and N. G. Hatsopoulos, "Kinetic trajectory decoding using motor cortical ensembles," *IEEE Trans. Neural Syst. Rehabil. Eng*, vol. 14, pp. 487-96, 2009.

[8] A. J. Suminski, D. C. Tkach, A. H. Fagg, and N. G. Hatsopoulos, "Incorporating feedback from multiple sensory modalities enhances brain-machine interface control," *J Neurosci*, vol. 30, pp. 16777-87, 2010.

[9] E. J. Cheng and S. H. Scott, "Morphometry of macaca mulatta forelimb. I. Shoulder and elbow muscles and segment inertial parameters," *J. Morphol.*, vol. 245, pp. 206–224, 2000.